Model for Pure Source Flow Chemical Lasers

Kerry E. Patterson,* Jad H. Batteh,† and Steade S. Howie‡
Science Applications, Inc., Atlanta, Georgia

A computationally efficient model is developed for the coupled gasdynamics and kinetics in a pure source flow chemical laser. Average flow properties are calculated using the one-dimensional equations for flow with area expansion and heat release. The flame sheet approximation is used to describe the mixing, and subsequent reaction, of the fuel and oxidizer streams. The gasdynamic properties of the mixed zone are assumed to be related in a simple way to the average flow properties. Application of the model to an HF laser indicates that the chemical efficiency of the laser is increased by increasing the nozzle exit Mach number, decreasing the initial source flow radius, decreasing the throughput, and increasing the mixing rate.

I. Introduction

IN recent years considerable effort has been expended in the development of chemical lasers because of their potential as efficient sources of laser radiation.[1] The source flow chemical laser, in particular, has emerged as a promising candidate for achieving high-power, continuous wave (cw) lasing. The advantage of the source flow concept lies in its use of an expanding flowfield to limit the temperature and pressure rise in the cavity, thereby allowing the laser to operate at low diluent levels.

In this paper we will focus on the chemically pumped cw HF laser. The particular source flow laser we will investigate is shown in Fig. 1. This design, which is characteristic of concepts proposed by the TRW Defense and Space Systems Group, consists of a series of supersonic oxidizer streams which enter the laser cavity from an array of source flow nozzles. The nozzles are fed by combustors in which the atomic fluorine is generated. As the oxidizer stream expands into the laser cavity, it mixes with the laser fuel (H_2 in this case) which is injected sonically from wedges placed at the nozzle exit. The exothermic reaction resulting from the mixing of the two streams creates the vibrationally excited HF. Thus, in this design mixing of the reactants occurs in a plane orthogonal to the expansion plane of the flow.

Detailed treatments[2,3] of source flow concepts have been developed but their complexity and lengthy computation time limit their utility for exploring wide ranges of geometry and operating conditions. On the other hand, simple models such as those developed by Mirels[4] and Grohs and Emanuel[5] have led to useful, simple scaling laws for chemical laser performance but they do not account for the streamwise variations in the flowfield which occur due to flow expansion and heat addition. The model described in this paper lies between these two extremes in that we use a coupled, albeit simplified, model for the gasdynamics and lasing kinetics in the cavity.

In this analysis, the effect of the base region between nozzles on laser performance is ignored. In other words, the distance between nozzle centerlines is assumed to be large enough that there is no mutual interaction between the flows of adjacent nozzles until some point downstream of where lasing has terminated. Until this point is reached, the cavity flowfield is assumed to retain a pure source flow character. The base region between adjacent source flows is modeled simply as a zero-gain region. In reality, however, the pressure in the base region will differ from the pressure in the source flow, leading to deviations from pure source flow behavior. An analysis of this effect is presented elsewhere.[6]

This paper is organized as follows. In Sec. II, we develop the basic gasdynamic and lasing equations for our model of an HF pure source flow chemical laser. We illustrate the use of the model in Sec. III where we investigate the effects of geometry and nozzle exit conditions on lasing efficiency. Section IV presents a summary of the paper and discussion of our results.

II. Theory

We assume that the physical characteristics and exit conditions of the nozzles in Fig. 1, as well as the mixing properties for each nozzle, are identical. Thus, we focus on the single segment shown in Fig. 2. In the expansion (r-z) plane, this segment is bounded by the nozzle centerline and the centerline of the base between nozzles. In the transverse (r-y) or mixing plane the segment is bounded by the wedge centerline and the centerline between wedges. In Fig. 2, θ denotes the source flow half-angle, r_i is the flow radius at the nozzle exit, h is half the distance between nozzles, and w is half the distance between wedges.

A. Gasdynamic Analysis

The flow in the mixing plane at each streamwise location, defined by the coordinate r, consists of three regions—an unmixed fuel stream, an unmixed oxidizer stream, and a region between the two where the two streams have mixed. To avoid the computational difficulty of solving separate gasdynamic equations for these three regions, we calculate an "average" set of gasdynamic properties for the entire flow. These average quantities are calculated based on an idealized flow whose properties are taken to be uniform in the y direction so that the gasdynamic properties between the nozzle centerline and flow boundary in Fig. 2 depend only on r. To initiate the calculations for this idealized flow, we assume that the fuel and oxidizer streams mix instantaneously, without reacting, at the nozzle exit plane. To account for the finite rate at which the two streams actually mix, chemical reactions are assumed to be confined to only a portion of the idealized stream, denoted as the mixed zone, which lies within the flame sheet boundary y_f shown in Fig. 2. The gasdynamic properties of the mixed zone, which control the chemical reaction rates, are assumed to be related in a simple way to the average flow properties, as discussed in Sec. II.B. However, the heat released by chemical reactions at any streamwise location is added to the entire idealized flow at the corresponding value of r.

Submitted Dec. 3, 1981; presented as Paper 82-0400 at the AIAA 20th Aerospace Sciences Meeting, Orlando, Fla., Jan. 11-13, 1982; revision received May 3, 1982. Copyright © American Institute of Aeronautics and Astronautics, Inc., 1982. All rights reserved.

*Staff Scientist. Member AIAA.
†Staff Scientist.
‡Division Manager.

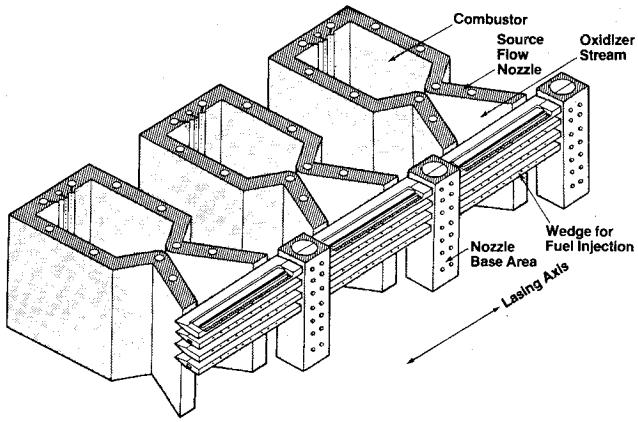

Fig. 1 Source flow chemical laser concept.

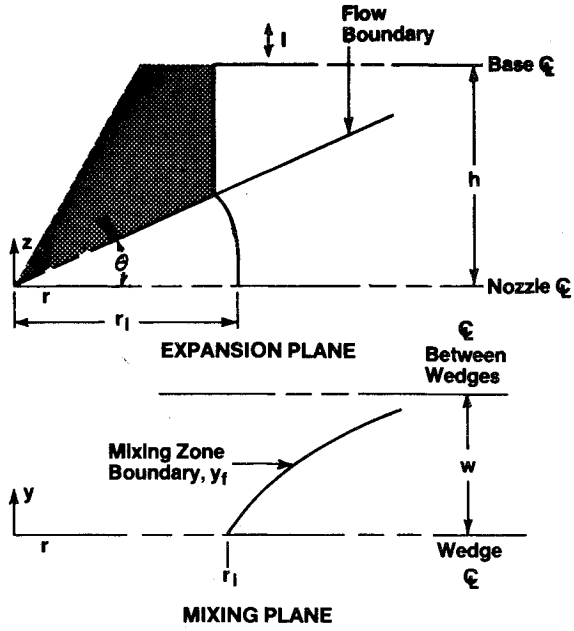

Fig. 2 Geometry for pure source flow laser analysis.

With these assumptions, the idealized flow is essentially a pure source flow with heat addition, and its gasdynamic properties are defined by[7]

$$\frac{dM^2}{dr} = \frac{M^2}{1-M^2}\left(1+\frac{\gamma-1}{2}M^2\right)\left[-\frac{2}{r}+\frac{1+\gamma M^2}{T_0}\frac{dT_0}{dr}\right] \quad (1)$$

$$\frac{p}{p_i} = \frac{r_i M_i}{rM}\left[\frac{\left(1+\frac{\gamma-1}{2}M_i^2\right)T_0}{\left(1+\frac{\gamma-1}{2}M^2\right)T_{0_i}}\right]^{1/2} \quad (2)$$

$$\frac{T}{T_i} = \frac{T_0}{T_{0_i}}\left[\frac{1+\frac{\gamma-1}{2}M_i^2}{1+\frac{\gamma-1}{2}M^2}\right] \quad (3)$$

$$\frac{\rho}{\rho_i} = \frac{pT_i}{p_i T} \quad (4)$$

In Eqs. (1-4), M is the flow Mach number, γ the ratio of specific heats, p the pressure, T the temperature, T_0 the total temperature, and ρ the density. The subscript i denotes the initial value of the variable, i.e., the value at the nozzle exit plane. In writing these equations, we have neglected the effect of temperature change and chemical reaction on the specific heats. A relationship which we shall find useful in the following sections is

$$\rho V r = \rho_i V_i r_i = \dot{m}/\theta \quad (5)$$

where $\dot{m}$ is the mass flow rate per unit length of nozzle. Equation (5) is, of course, just a statement of mass continuity for source flows.

The gasdynamics of the laser cavity, as expressed by Eqs. (1-4), is influenced by the chemical kinetics because the total temperature increases due to the thermal energy released by the pumping and collisional deactivation reactions. An expression for T_0 will be derived from the lasing analysis in Sec. II.C.

B. Mixed Zone Analysis

The gasdynamic interactions occurring between the fuel and oxidizer streams at the nozzle exit and during the mixing process are extremely complex and difficult to analyze in detail.[5] The pressure in the sonic fuel stream as it enters the laser cavity is generally several orders of magnitude greater than the pressure in the supersonic oxidizer stream. As the two streams enter the laser cavity and begin mixing, the fuel stream expands to achieve pressure equilibrium with the oxidizer stream. The impact of this initial pressure mismatch on the mixing in the laser cavity has not been treated in detail. Instead, it is generally assumed that pressure equilibration occurs instantaneously at the nozzle exit before any appreciable mixing has occurred. This assumption has also been used in our analysis since we calculate the average gasdynamic properties at the nozzle exit by instantaneously mixing the two streams and bringing them to a common gasdynamic state.

To evaluate the thermodynamic properties of the mixed zone we introduce a number of assumptions which allow us to relate the mixed zone properties to the average gasdynamic properties of the flow. Although the mixed zone properties derived from our analysis do not strictly satisfy the conservation laws (in particular, the momentum and energy equations are not satisfied), they hopefully represent a reasonable approximation to the actual properties in the mixed zone. It should be noted that the mixed zone properties are used primarily to define the temperature and pressure for calculating the reaction and lasing rates. The average gasdynamic properties, on the other hand, are calculated from the conservation equations and, as such, represent a consistent solution, at least for the idealized flow problem.

The mixed zone between the fuel and oxidizer streams is assumed to grow according to the power law relation

$$y' \equiv y_f/w = (x/\ell_m)^m \quad (6)$$

where $x = r - r_i$ represents the radial distance from the nozzle exit and ℓ_m, the mixing length, denotes the distance downstream from the nozzle exit where the fuel and oxidizer streams are fully mixed, i.e., where $y' = 1$. For $x > \ell_m$, the width of the mixed zone is, of course, kept fixed at $y' = 1$. The exponent m is generally taken to be ½ and 1 for laminar and turbulent mixing, respectively.

The mixing length depends on the diffusion coefficients of the two streams, their gasdynamic properties, and on the wedge spacing. For example, ℓ_m varies as $w^2\rho V/T^{1/2}$ for laminar mixing.[5] The mixing length may be artificially shortened, however, through a variety of mixing enhancement schemes. Since one purpose of this analysis will be to determine the effect of mixing length on laser performance, we will treat ℓ_m as an independent variable.

Since the chemical reactions are confined to the mixed zone, it is necessary to relate the mixed zone properties to the

average gasdynamic properties, derived in the preceding section, in order to calculate the reaction rates. To do this, we assume that pressure equilibration between the mixed and unmixed regions of the flow occurs instantaneously. Thus, if we denote mixed zone properties by the subscript m, we have

$$p_m = p \tag{7}$$

where p is the average pressure obtained from Eq. (2). In addition, we assume that the mass flux is uniform in the region between the wedges so that

$$\rho_m V_m = \rho V = \dot{m}/r\theta \tag{8}$$

where the last relationship is obtained from Eq. (5). Although Eq. (8) is commonly used in conjunction with the flame sheet approximation,[4,8] it is strictly valid only when the flow is incompressible and isobaric. Its use is generally justified, as in our case, because it provides a convenient method of estimating mixed zone properties.

In specifying the mixed zone temperature, it is necessary to account for the fact that near the nozzle exit the mixed zone temperature is higher than the average source flow temperature because the oxidizer stream initially entrained into the mixing layer originates from the boundary layer of the flow over the wedges. As more flow is entrained into the mixed zone, the influence of the initial boundary-layer temperature on the mixed zone temperature diminishes. In fact, once the two streams are fully mixed, then the mixed zone comprises all of the flow and the temperature in the mixed zone must equal the average gasdynamic temperature T defined by Eq. (3). To reflect this variation in a simple manner, we assume that the mixed zone temperature T_m is the weighted average of the initial mixed zone temperature T_{m_i} and the average temperature T according to

$$T_m = T_{m_i} + y'(T - T_{m_i}) \tag{9}$$

The initial mixed zone temperature, which is considered an input in this analysis, can be obtained either from experiments or from a boundary-layer calculation of the flow of the oxidizer stream over the wedges.

The mixed zone density can now be determined from the equation of state

$$\rho_m = \bar{M} p_m / R_u T_m \tag{10}$$

where R_u is the universal gas constant and $\bar{M}$ is the average molecular weight of the mixed streams. For the reactions considered here the number of moles remains constant, so that the average molecular weight is unchanged by chemical reactions.

The mixed zone concentration of a species S is defined by the species conservation equation

$$\frac{\mathrm{d}}{\mathrm{d}r}(\rho_m V_m r y' C_{s_m}) = r y' \dot{\omega}_{s_m} \tag{11}$$

where V_m is the source flow velocity in the mixed zone, C_{s_m} the mass fraction of species S in the mixed zone, and $\dot{\omega}_{s_m}$ the rate of change of species S per unit volume of the mixed zone due to chemical reactions.

For a uniform mass flux between the wedges, the mass fraction in the mixed zone is related to the flow average mass fraction C_s by

$$C_s = (1 - y') C_{s_i} + y' C_{s_m} \tag{12}$$

where C_{s_i} is the mass fraction of species S at the nozzle exit.

Substituting Eqs. (8) and (12) into Eq. (11) yields

$$\frac{\mathrm{d}}{\mathrm{d}r}[C_s - (1 - y') C_{s_i}] = \frac{r\theta}{\dot{m}} y' \dot{\omega}_{s_m} \tag{13}$$

for the species conservation equation. Equation (13) is actually a flow average species conservation equation which complements Eqs. (1-4) for the average gasdynamic properties. The effect of the mixed zone is included in the production term since $\dot{\omega}_{s_m}$ is evaluated at the mixed zone properties and y' limits the fraction of the flow which can react.

In this analysis we will be concerned with the HF laser pumped by the reaction

$$\mathrm{F} + \mathrm{H_2} \rightarrow \mathrm{HF}(v) + \mathrm{H} \tag{14}$$

where $v = 0$-3 represents the vibrational level of the HF molecule generated by the reaction. If we denote by C_{HF} the flow average mass fraction of all the HF, regardless of vibrational level, then we can relate the mass fraction of the reacting species to C_{HF} by the equations

$$C_{\mathrm{F}} = C_{\mathrm{F}_i} - M_{\mathrm{F}} C_{\mathrm{HF}} / M_{\mathrm{HF}} \tag{15}$$

$$C_{\mathrm{H_2}} = C_{\mathrm{H_{2i}}} - M_{\mathrm{H_2}} C_{\mathrm{HF}} / M_{\mathrm{HF}} \tag{16}$$

$$C_{\mathrm{H}} = M_{\mathrm{H}} C_{\mathrm{HF}} / M_{\mathrm{HF}} \tag{17}$$

where M_s is the molecular weight of species S.

The rate of production of HF in the mixing zone is given by

$$\dot{\omega}_{\mathrm{HF}_m} = \frac{\rho_m^2 C_{\mathrm{F}_m} C_{\mathrm{H_2}_m} M_{\mathrm{HF}}}{M_{\mathrm{F}} M_{\mathrm{H_2}}} k_p(T_m) \tag{18}$$

where k_p is the reaction rate for the pumping reaction in cm^3/mole·s. Consistent with our preceding discussion, k_p is evaluated at the mixed zone temperature.

For most chemical lasers of interest, the reaction is fuel rich and it is instructive to write the pumping equation in terms of the pumping parameter

$$X_T = M_{\mathrm{F}} C_{\mathrm{HF}} / M_{\mathrm{HF}} C_{\mathrm{F}_i} \tag{19}$$

which represents the ratio of the number of moles of HF created to the number which would be generated if all the F atoms had reacted. Thus, X_T always lies between zero and unity, approaching unity for the fuel rich case as the pumping reaction goes to completion.

If, in addition, we define the laser fuel ratio

$$R_L = 2X_{\mathrm{H_{2i}}} / X_{\mathrm{F}_i} \tag{20}$$

where $X_{\mathrm{H_{2i}}}$ and X_{F_i} are the initial mole fractions of $\mathrm{H_2}$ and F in the mixed streams, then Eq. (18) can be rewritten as

$$\dot{\omega}_{\mathrm{HF}_m} = \frac{\rho_m^2 X_{\mathrm{F}_i} X_{\mathrm{H_{2i}}} M_{\mathrm{HF}}}{\bar{M}^2} k_p(T_m) \left(1 - \frac{X_T}{y'}\right)\left(1 - \frac{2X_T}{R_L y'}\right) \tag{21}$$

In writing Eq. (21), we have used Eqs. (12), (15), and (16) to relate the mixed zone concentrations of the reactants to their initial values and to the global concentration of HF. In addition, we have used the relationship

$$C_s = M_s X_s / \bar{M} \tag{22}$$

to relate the average mass fraction of species S to its average mole fraction.

Substituting Eqs. (19) and (21) into Eq. (13), and using the initial condition $C_{\mathrm{HF}_i} = 0$, yields

$$\frac{\mathrm{d}X_T}{\mathrm{d}r} = A_p r \rho_m^2 k_p(T_m) y' \left(1 - \frac{X_T}{y'}\right)\left(1 - \frac{2X_T}{R_L y'}\right) \tag{23}$$

where

$$A_p = \theta X_{\mathrm{H_{2i}}} / \dot{m} \bar{M} \tag{24}$$

is a constant. Equation (23) describes the evolution of the HF concentration in the laser cavity due to mixing and the subsequent reactions in the mixed zone.

C. Lasing Analysis

The pumping reaction, represented by Eq. (14), creates HF molecules which are excited up to the $v=3$ vibrational level. Lasing then occurs on transitions involving adjacent vibrorotational levels. In our analysis we will assume that the population of the rotational levels within each vibrational level is characterized by an equilibrium distribution at the mixed zone temperature. Since the initial pumping reaction produces HF molecules which are not in rotational equilibrium,[9] this assumption is valid only if the rate of rotational relaxation due to collisional deactivation is much faster than the rate of stimulated emission. At the pressures typical of source flow chemical lasers (~ 10 Torr), collisional deactivation is inhibited and it is likely that lasing performance will be influenced somewhat by the rotational nonequilibrium of the lasing species.

The effect of rotational nonequilibrium on chemical laser performance has been investigated analytically by several investigators. (See, for example, Refs. 10 and 11.) These analyses suggest that the differences between the rotational equilibrium and nonequilibrium models are not so much in their predictions of the total output power (the rotational equilibrium model tends to overpredict the power by approximately 15-30%) as in the predictions of the spectral distribution of that power. Since, in this analysis, we are concerned with establishing trends in the total power, rather than the spectrum, we will impose the rotational equilibrium assumption. It should be mentioned that there is a problem in incorporating a rotational nonequilibrium model, aside from the obvious increase in computation time required, because the rotational relaxation rates for many collision partners are not accurately known.

For the lasing analysis, we assume a Fabry-Perot optical cavity with lasing only on P-branch transitions. The notation g_v and I_v will designate the gain and intensity, respectively, for the transition $(v+1,\ J-1 \rightarrow v,\ J)$. We will assume, in addition, that the rotational quantum number for the transition, denoted by the value of J, is the same for all transitions and does not vary with distance downstream from the nozzle. Our derivation of the lasing equations will parallel that of Mirels,[4] who, in turn, used a procedure similar to that of Broadwell[12] and Emanuel and Whittier.[13] Mirels showed that the total output power of a Fabry-Perot cavity operating on several transitions could be represented by a single equation if the gain is taken to be the same for all lasing transitions, and if lasing is assumed to be initiated, and terminated, simultaneously for all transitions. The analysis presented in this section will actually be an extension of that of Mirels since we will allow for streamwise variations of the gasdynamic variables, and in addition we will include the effect of multiquantum deactivation.

For our source flow treatment to remain strictly valid in the presence of a radiation field, the intensity of the radiation would have to be a function only of the radial coordinate. This requires that the radiation path in the source flow region coincide with source flow arcs and also that the gain times the arc length be much less than unity so that we can neglect the effect of amplification on the magnitude of the intensity as it traverses the arc. If these two conditions are satisfied, the power P derived from the single mixing segment shown in Fig. 2 can be obtained from the equation

$$\frac{dP}{dr} = \left[\sum_{v=0}^{v_f-1} g_{v_m}(r) I_v(r) \right] y_f r\theta$$

where g_{v_m} is the gain in the mixed zone for the $v+1 \rightarrow v$ transition, I_v the corresponding intensity, and v_f the highest vibrational level which participates in the lasing. The arc length $r\theta$ represents the gain length for the ray at radius r.

The condition on the gain required for the above equation to be valid is generally satisfied for chemical lasers of interest. In fact, we will impose the more stringent requirement that the gain times the array length in the lasing direction is much less than unity so that each nozzle in the array will be exposed to essentially the same radiation field. The first condition, however, poses a problem since the intensity field is really a function of x and not r. To retain the source flow formalism, we assume that I_v can be represented as a function of r but in calculating the power we use the chord $r\sin\theta$ rather than the arc length as the gain length. Thus, we approximate the power by the equation

$$\frac{dP}{dr} = \left[\sum_{v=0}^{v_f-1} g_{v_m}(r) I_v(r) \right] y_f r\sin\theta \tag{25}$$

Equation (25) should represent a reasonable approximation for the lasing power which can be extracted for moderate source flow angles.

A useful parameter for evaluating lasing efficiency in fuel-rich HF lasers is the chemical specific efficiency η defined as

$$\eta = P/\dot{m} C_{F_i} w \tag{26}$$

η is a measure of the energy extracted from the laser per gram of fluorine flowing through the cavity. Equation (25) can be written in terms of η as

$$\frac{d\eta}{dr} = \frac{y' r\sin\theta}{\dot{m} C_{F_i}} \sum_{v=0}^{v_f} g_{v_m} I_v \tag{27}$$

The gain in Eq. (27) is by assumption independent of the vibrational level and its value is calculated based on a gain equals loss condition for the cavity. To facilitate comparison with the analysis of Ref. 6, it is convenient to define a threshold gain g_{th} based on the height h between the nozzle centerline and the base centerline (see Fig. 2):

$$g_{th} = -\frac{\ell n(R_1 R_2)}{4 N_n h} \tag{28}$$

where R_1 and R_2 are the reflectivities of the mirrors bounding the cavity and N_n denotes the number of primary nozzles in the array. If the wedges in adjacent nozzles were perfectly aligned, then the intensity profile as a function of y would extend only to the edge of the flame sheet for each mixing layer. For that case, the gain in the mixing layer required to support lasing is given by

$$g_{v_m} = g_{th} \frac{h}{r\sin\theta}$$

More often, however, the wedges in adjacent nozzles are offset or canted to provide a more uniform lasing medium. In that case the intensity profile fills the entire region between the wedges and a simple calculation shows that the gain must satisfy

$$g_{v_m} = \frac{g_{th} h}{y' r\sin\theta} \tag{29}$$

Equation (29) merely states that for offset wedges the gain in the mixed zone must be increased by the factor $1/y'$ since the radiation passing through the mixed zone of one nozzle will also pass through the unmixed zone of a subsequent nozzle. In our analysis we will use Eq. (29) to define the gain for the Fabry-Perot cavity.

Equation (29) defines the gain in the mixed zone whenever lasing is occurring. Since the gain is initially zero at r_i, there will be a region adjacent to the nozzle exit where the intensity is zero and the gain increases to achieve threshold. Once the gain in the medium achieves the value specified by Eq. (29), lasing is initiated. At some point downstream, the gain in the medium will be insufficient to satisfy Eq. (29) and lasing will terminate.

It is interesting to note that the gain specified by Eq. (29) as well as the threshold gain condition [Eq. (28)] can both be expressed in terms of the product of h and g_{th}. Thus, in the calculations of Sec. III we will specify the product hg_{th} and adjust h to prevent the source flows of adjacent nozzles from impinging.

The sum in Eq. (27), which represents the sum of the power from each lasing transition, is evaluated from the species conservation equation for the individual vibrational levels of HF. If we denote the mass fraction of HF in the vth vibrational level by C_v, then we can write a flow average species conservation equation according to Eq. (13),

$$dC_v/dr=\theta r y'[a_p(v)\dot{\omega}_{HF_m}+\dot{\omega}^v_{CD_m}+\dot{\omega}^v_{R_m}]/\dot{m} \tag{30}$$

where $a_p(v)$ represents the fraction of HF pumped into the vth vibrational level, $\dot{\omega}_{HF_m}$ is the rate of production of HF in the mixed zone [given by Eq. (18)], and $\dot{\omega}^v_{CD_m}$ and $\dot{\omega}^v_{R_m}$ represent the rate of change of C_v due to collisional deactivation and radiation, respectively.

Explicitly, $\dot{\omega}^v_{CD_m}$ is given by the expression

$$\dot{\omega}^v_{CD_m}=\rho_m^2\sum_S\frac{C_{S_m}}{M_S}\left[-C_{v_m}\sum_{v'=0}^{v-1}k_S^{v,v'}(T_m)+\sum_{v'=v+1}^{v_f}C_{v'_m}k_S^{v',v}(T_m)\right] \tag{31}$$

where $k_S^{v,v'}(T_m)$ is the rate for the collisional deactivation reaction

$$HF(v)+S\rightarrow HF(v')+S \tag{32}$$

The outer sum in Eq. (31) is over all species in the flow. In writing Eq. (31), we are assuming that there is no dependence on the vibrational level of the deactivating partner. To simplify Eq. (31) we assume that each species S has a single quantum rate and a multiquantum rate such that

$$k_S^{v,v'}(T_m)=k_S^{sq}(T_m)g_{sq}(v)+k_S^{mq}(T_m)g_{mq}(v),v'=v-1$$
$$=k_S^{mq}(T_m)g_{mq}(v),v'\le v-2 \tag{33}$$

According to Eq. (33), each species has its own absolute rate, but the scaling of the rates with vibrational level, defined by $g_{sq}(v)$ and $g_{mq}(v)$, is taken to be the same for all species.

The radiation term in Eq. (30) is given by

$$\dot{\omega}^v_{R_m}=\frac{M_{HF}}{\epsilon}(g_{v_m}I_v-g_{v-1_m}I_{v-1}) \tag{34}$$

where $\epsilon=4.54\times10^4$ J/mole is the energy difference between adjacent vibrational levels for HF (assumed to be independent of v). The gain in the mixed zone is evaluated from

$$g_{v_m}=\rho_m\sigma_v[C_{v+1_m}-AC_{v_m}]/M_{HF} \tag{35}$$

The gain cross section in Eq. (35) can be evaluated from[4]

$$\sigma_v=C_\sigma T_m^{-3/2}(1+v-0.01v^3)(1+0.063J)Je^{-J(J-1)T_R/T_m} \tag{36}$$

where $C_\sigma=4.26\times10^{11}$ cm^2-K$^{3/2}$/mole and T_R, the characteristic rotational temperature, is 30.16 K. The parameter A in Eq. (35) is given by

$$A=\exp[-2JT_R/T_m] \tag{37}$$

In this analysis, we neglect the effect of the source flow on line shape, which is justified for the operating conditions we will investigate (modest M_i, low g_{th}). At high Mach numbers and high threshold gains, the effect of Doppler broadening of the line profile results in a decrement in the laser output power.[14,15]

After substitution of Eq. (34) for the radiation term, Eq. (30) can be solved sequentially for the product g_vI_v for each lasing transition. Summing over all transitions yields the relationship

$$\sum_{v=0}^{v_f-1}g_{v_m}I_v=\frac{\epsilon}{M_{HF}}\left\{\frac{\dot{m}}{y'r\theta}\sum_{v=0}^{v_f}v\left[a_p(v)\frac{dC_{HF}}{dr}-\frac{dC_v}{dr}\right]-\sum_{v=0}^{v_f}\sum_{v'=0}^{v}\dot{\omega}^{v'}_{CD_m}\right\} \tag{38}$$

Equation (38) provides an expression for the sum necessary to evaluate Eq. (27) for the chemical specific efficiency. As it stands, however, the sum cannot be evaluated without first solving the species equations for each vibrational level of HF since the C_v appear explicitly in the equation. If, however, the gain on all lasing transitions is taken to be the same, Eq. (35) can be solved explicitly for C_v in terms of the total mass fraction of HF and the common gain with the result that[4]

$$C_v=F_vC_{HF}+H_v\beta \tag{39}$$

where

$$F_v=\frac{A^v(A-1)}{A^{v_f+1}-1} \tag{40}$$

$$H_v=A^{v-1}\sum_{i=0}^{v-1}\frac{\sigma_0/\sigma_i}{A^i}-F_v\sum_{v=0}^{v_f-1}\left[\frac{\sigma_0}{\sigma_v}\sum_{i=0}^{v_f-1-v}A^i\right] \tag{41}$$

$$\beta=\frac{g_m y' M_{HF}}{\rho_m\sigma_0} \tag{42}$$

In defining β, we have replaced the symbol g_{v_m} for the gains in the mixed zone with the symbol g_m to denote that the gain is independent of the vibrational level.

Substituting Eqs. (38) and (39) into Eq. (27) and writing the collisional deactivation term explicitly yields, after some algebraic simplification, the following equation for the chemical specific efficiency:

$$\frac{d\eta}{dr}=\frac{d}{dr}(\eta_{max}X_T-S_1)-DX_T-S_2 \tag{43}$$

where

$$\eta_{max}=\frac{\epsilon\sin\theta}{M_F\theta}\sum_{v=0}^{v_f}v[a_p(v)-F_v] \tag{44}$$

$$S_1=\frac{\epsilon\sin\theta}{C_{F_i}\theta}\left(\frac{g_m y'}{\rho_m\sigma_0}\right)\sum_{v=0}^{v_f}vH_v \tag{45}$$

$$D=\frac{\epsilon\sin\theta}{\dot{m}M_F}\rho_m^2 r\sum_S\frac{C_{S_m}}{M_S}\sum_{v=0}^{v_f}F_vk_{Sv} \tag{46}$$

$$S_2=\frac{\epsilon\sin\theta}{\dot{m}C_{F_i}}\left(\frac{\rho_m r g_m y'}{\sigma_0}\right)\sum_S\frac{C_{S_m}}{M_S}\sum_{v=0}^{v_f}H_vk_{Sv} \tag{47}$$

$$k_{Sv}=k_S^{sq}(T_m)g_{sq}(v)+\tfrac{1}{2}v(v+1)k_S^{mq}(T_m)g_{mq}(v) \tag{48}$$

In writing Eq. (43) we have substituted Eqs. (31) and (33) into the collisional deactivation term and used Eq. (19) to write C_{HF} in terms of the pumping parameter X_T.

Equation (43) is the source flow counterpart to Eq. (25a) of Mirels' analysis[4] generalized to include streamwise variations in the gasdynamic parameters and multiquantum deactivation processes. According to Eq. (43), the chemical specific efficiency can be written in terms of the pumping parameter and four additional parameters which have clear physical meanings. η_{max} represents the maximum chemical specific efficiency which can be achieved at r. It corresponds to the case of a fully pumped ($X_T = 1$), saturated laser ($g_{th} = 0$) with no collisional deactivation ($D = 0$). The parameters S_1, D, and S_2 represent the loss in chemical specific efficiency due to collisional deactivation and saturation effects. S_1, which represents the decrement in the efficiency due to finite gain, arises because the populations of the excited vibrational levels required to maintain a value of g increase with g. Thus, less energy is available for lasing. Likewise, collisional deactivation reduces the lasing energy and this effect is represented by the last two terms in Eq. (43).

If we define r_t as the radius where the lasing threshold condition [Eq. (29)] is first achieved, then $\eta = 0$ for $r < r_t$ and Eq. (43) defines the evolution of the gain g_m as a function of r. For $r \geq r_t$, g is given by Eq. (29) and Eq. (43) is used to obtain η as a function of r. Termination of lasing occurs at the cutoff radius r_{co} defined as the radius where $d\eta/dr = 0$. For $r > r_{co}$, η is constant and Eq. (43) once again defines the mixed zone gain. The solution of Eq. (43) is facilitated by writing it as a differential equation for the variable $\eta - \eta_{max} X_T + S_1$. Since this parameter varies smoothly with r, this reformulation avoids the numerical difficulties encountered at $r = r_t$ where $d\eta/dr$ and dg/dr are discontinuous.

We can now evaluate the term in Eq. (1) corresponding to the increase in total temperature of the source flow. The total temperature change is given by

$$\frac{dT_0}{dr} = \frac{C_{F_i}}{c_p}\left(\frac{dQ_p}{dr} + \frac{dQ_{CD}}{dr}\right) \tag{49}$$

where c_p is the specific heat per unit mass for the mixed streams, and dQ_p/dr and dQ_{CD}/dr represent the thermal energy added to the flow, in J/g-F, due to the pumping reaction and collisional deactivation, respectively. Specifically,

$$\frac{dQ_p}{dr} = \left[H - \epsilon \sum_{v=0}^{v_f} v a_p(v)\right] \frac{1}{M_F} \frac{dX_T}{dr} \tag{50}$$

where $H = 1.27 \times 10^5$ J/mole is the heat of reaction for the pumping reaction. The energy deposited due to collisional deactivation is given by the last two terms in Eq. (43), namely,

$$\frac{dQ_{CD}}{dr} = DX_T + S_2 \tag{51}$$

Substituting Eqs. (50) and (51) into Eq. (49) and using Eq. (43) yields

$$T_0 = \frac{C_{F_i}}{c_p}\left\{\frac{1}{M_F}\left[H - \epsilon \sum_{v=0}^{v_f} v a_p(v)\right] X_T + \eta_{max} X_T - S_1 - \eta\right\} + T_{0_i} \tag{52}$$

for the total temperature of the source flow.

The assumptions introduced in these three subsections have allowed us to reduce the equations for a cw, pure source flow chemical laser to essentially three coupled, ordinary differential equations—Eq. (1) for the average flow Mach number, Eq. (23) for the pumping parameter X_T, and Eq. (43) for the chemical specific efficiency. These three equations can be readily solved using a number of standard techniques. In our analysis, we use a fourth-order Runge-Kutta scheme. It is worth noting that for most cases of interest the rate of creation of HF is limited primarily by the mixing of the reactants. In that case, the solution of the equations is expedited considerably by transforming the independent variable from r to y' through Eq. (6).

III. Application of the Model

In this section, we will illustrate how the model developed in Sec. II can be used to study the effect of geometry and nozzle exit conditions on laser performance. For this illustration we will take the values shown in Table 1 as baseline conditions. The initial flow radius of 4.64 cm and source flow half-angle $\theta = 22$ deg are typical for a source flow laser nozzle. The baseline gasdynamic properties were obtained from a detailed combustor and viscous nozzle-wedge calculation for a typical operating point. T_{m_i} was taken to be the average temperature in the boundary layer of the oxidizer stream at the trailing edge of the wedge. The numerical value of T_{m_i} shown in the table was obtained from a boundary-layer analysis for a typical wedge geometry.

In the following discussion we will investigate the effect on η of varying either the initial Mach number, the initial radius, or the mass flux $\rho_i V_i$ independently, while keeping the other parameters fixed at their baseline values. In each case, the efficiency will be plotted as a function of the mixing length. Laminar growth of the mixed zone, corresponding to $m = \frac{1}{2}$ in Eq. (6), was assumed in these calculations. The reaction rates used in the analysis are detailed in Ref. 16.

The chemical specific efficiency was calculated over a range of values of the rotational quantum number for each case. The value of η reported for the parametric studies corresponds to the J which maximized η for each particular set of parameters. For most of the cases, this value of J was either 9 or 10, although a J as high as 12 was required to maximize η for some of the shorter mixing lengths.

It is worth noting that in these calculations we have taken $v_f = 2$ so that we consider only two lasing transitions, even though the pumping reaction populates up to the third excited vibrational level. Detailed calculations with a multiline model indicate that the $v = 3$ to $v = 2$ transition is able to lase only for very low gains and, even then, only near the nozzle exit. Lasing on the 2 to 1 and 1 to 0 transitions is considerably stronger and these lines have a much longer cutoff radius. This difference in behavior occurs because the initial vibrational distribution due to the pumping reaction is much more favorable for lasing from the lower two levels. Because of the common gain assumption, we are unable to terminate lasing independently for each transition. If we keep the 3 to 2 transition, a penalty in η is incurred because some of the energy available for lasing is taken from the 2 to 1 and 1 to 0

Table 1 Baseline conditions

Nozzle geometry	Threshold gain
$r_i = 4.64$ cm	$hg_{th} = 0.00078$
$\theta = 22$ deg	
Flow properties	Laminar mixing
$M_i = 3.26$	$m = 0.5$
$T_{0_i} = 1130$ K	
$\gamma = 1.47$	
$\rho_i v_i = 0.502$ g/cm$^2 \cdot$s	
$T_{m_i} = 561$ K	
$C_{F_i}/C_{H_{2i}}/C_{DF_i}/C_{He_i}/C_{N_{2i}}$	
$= 0.197/0.104/0.410/0.151/0.139$	

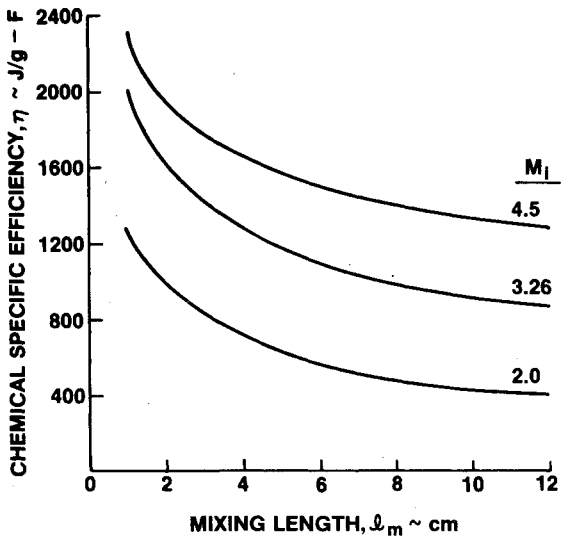

Fig. 3 Effect of initial Mach number on chemical specific efficiency.

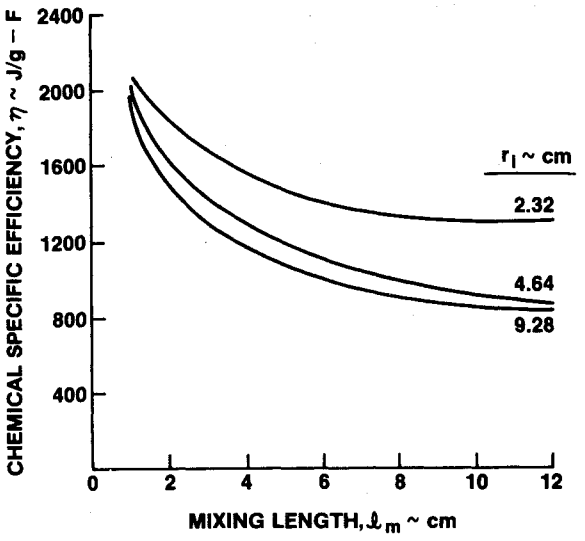

Fig. 4 Effect of initial source flow radius on chemical specific efficiency.

transitions in order to keep the gain on the 3 to 2 transition artificially high. Consequently, predictions of the common gain model for η generally fall far below the predictions of the multiline model if all three transitions are kept. On the other hand, if only the lowest two transitions are considered the common gain model approximates the multiline model quite well.

Figure 3 shows the effect of initial Mach number on chemical specific efficiency as predicted by the model. For a given Mach number, we note that η increases with decreasing ℓ_m. This occurs because at the longer mixing lengths lasing is terminated before mixing is complete so that a substantial fraction of the fluorine remains unreacted until after the lasing has cut off. As the mixing length decreases, the fraction of unreacted fluorine at cutoff is decreased and η increases. For example, for the baseline case with $\ell_m = 10$ cm, the pumping parameter X_T equals only 0.48 when lasing terminates at 2.5 cm from the nozzle exit. On the other hand, for a mixing length of 4 cm, lasing terminates at a shorter distance downstream, 1.96 cm, but by that distance X_T has reached a value of 0.68. This increase in the value of X_T is reflected in approximately a 40% increase in η, from 910 to 1270 J/g-F. For very short mixing lengths, on the order of 1-2 cm, nearly all the fluorine is mixed and reacted before cutoff occurs and we note a dramatic increase in chemical specific efficiency. The variation of η with ℓ_m demonstrated by the curves in Fig. 3 will be characteristic of all the cases we will consider.

Figure 3 also indicates an increase in lasing efficiency with increasing Mach number. This occurs primarily because, for a constant mass flux, a higher M_i corresponds to lower pressures and temperatures in the laser cavity. For example, for the baseline case the pressure and temperature at the nozzle exit are $p_i = 5.5$ Torr and $T_i = 320$ K, whereas for $M_i = 4.5$, $p_i = 3.1$ Torr and $T_i = 196$ K.

Figure 4 shows the effect on lasing efficiency of halving and doubling the baseline value of r_i. According to the figure, halving the source flow radius leads to an increase of about 50% in η at the longer mixing lengths. The reason for the enhancement is that the smaller radius nozzle provides greater area relief to maintain the lower temperatures and pressures favorable for lasing. Little difference is observed, however, between the $r_i = 4.64$ and 9.28 cm cases. The insensitivity arises because for these two cases lasing cuts off within 3.6 cm downstream of the nozzle exit. Thus, neither nozzle is really able to take advantage of the area relief provided by the source flow. This suggests that the nozzle radius should be chosen such that lasing terminates at $r_{co} \gtrsim 2r_i$ (or $x_{co} \gtrsim r_i$,

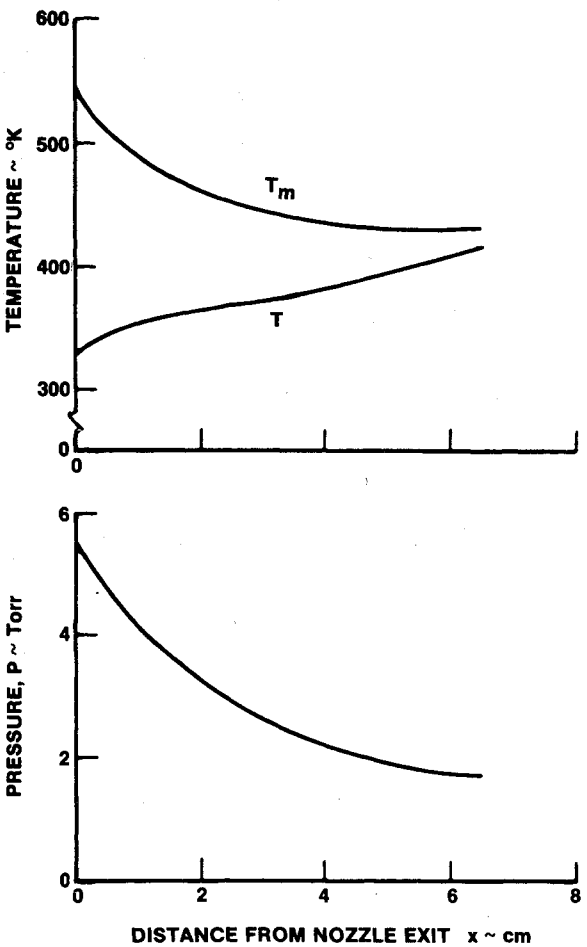

Fig. 5 Thermodynamic characteristics of a source flow laser ($r_i = 2.32$ cm, $\ell_m = 8$ cm).

where x_{co}, is the distance to the cutoff point measured from the nozzle exit). Figure 4 also shows that all three nozzles approach the same value of η as the mixing length is reduced, again because cutoff occurs at such a short distance from the nozzle exit that none of the nozzles is able to take advantage of the area expansion of the flow.

The trend of increasing chemical efficiency with decreasing r_i is generally valid, but the radius at which efficiency

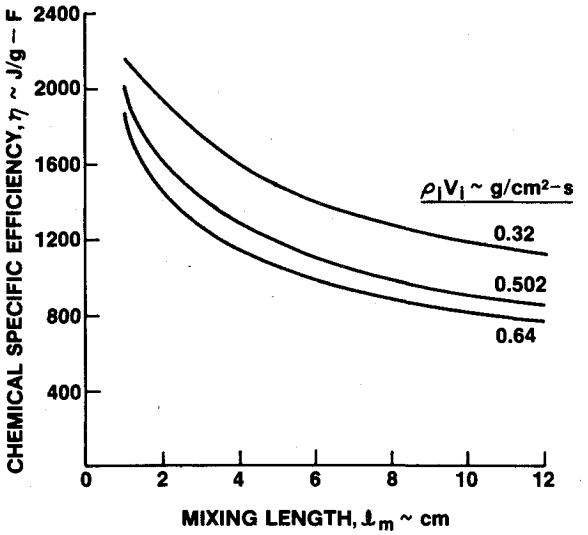

Fig. 6 Effect of throughput on chemical specific efficiency.

becomes insensitive to r_i depends on the flow conditions. For example, at lower throughput levels or higher diluent levels than those used to generate Fig. 4, x_{co} increases so that significant increases in the chemical efficiency can be obtained even for relatively large values of r_i.

The ability of small radius, source flow nozzles to maintain thermodynamic conditions favorable for lasing is illustrated graphically in Fig. 5. Here we have plotted the temperature and pressure profiles in the laser cavity as a function of distance from the nozzle exit for a source flow laser with $r_i = 2.32$ cm and a mixing length of 8 cm. The profiles are plotted out to x_{co} which corresponds to 6.5 cm for this case. Although the total temperature of the flow has increased by 20% by the time lasing cuts off, the area expansion provided by the source flow has limited the rise in T to only approximately 100 K and the pressure actually falls dramatically from 5.5 to 1.7 Torr. We have also plotted the variation of the mixed zone temperature as calculated by Eq. (9) for this case. It decreases monotonically from 561 K at the nozzle exit to approximately the average source flow temperature at x_{co}. The Mach number, although not shown in the figure, decreases only slightly from 3.26 at the nozzle exit to 3.11 at cutoff.

In Fig. 6 we show how the throughput influences η. The throughput changes were obtained by varying $\rho_i V_i$ while keeping the initial mass fractions fixed at the values specified in Table 1. In general, a decrease in chemical specific efficiency accompanies an increase in throughput. This occurs because the flow pressures and temperatures are higher for a higher throughput if the initial Mach number is kept fixed.

Figures 3-6 indicate that the chemical specific efficiency of a source flow chemical laser increases with increasing M_i, decreasing r_i, decreasing mixing length, and decreasing throughput. It should be mentioned, however, that increases in lasing efficiency may not necessarily result in increases in the laser output power. According to Eq. (26), the power is proportional not only to η but also to the product $\rho_i V_i r_i$ which represents the total flow rate per unit height of nozzle. Thus, increasing η by decreasing throughput or the initial source flow radius will result in a decrease in output power unless the increase in efficiency is sufficient to offset the decrease in the total flow rate.

IV. Summary

In this paper, we have developed a computationally efficient model for estimating the performance of source flow chemical lasers. The analysis assumes that the flow in the laser cavity can be described, in an average sense, by the equations describing a pure source flow with heat addition. The flame sheet approximation is used to define the growth of the mixed zone between the laser fuel and oxidizer streams. The properties of the mixed zone, which define the thermodynamic conditions for the lasing and chemical reactions, are related in a simple way to the average flow properties. The lasing performance of the cavity is determined by an extension of Mirels' analysis[4] which accounts for multiquantum deactivation of the lasing species and for variations in the flow properties with distance downstream.

The model is intended primarily to identify those nozzle exit conditions and flow geometries which have the potential for achieving high lasing performance. For the cases investigated, the model indicates that the chemical specific efficiency increases with increasing nozzle exit Mach number, decreasing initial flow radius, decreasing throughput, and faster mixing. In performing these optimization studies, it was assumed that each parameter could be varied independently. In practice these parameters are coupled so that changes in the nozzle design intended to alter the value of one parameter will likely affect some of the other parameters. For example, decreasing the radius of the nozzle will affect the gasdynamic conditions at the nozzle exit, even if the ratio of r_i to the throat height is kept fixed, because of the altered viscous properties of the smaller nozzle. These effects can be included, of course, when considering a specific nozzle-wedge configuration. Manufacturing and structural considerations also place a practical limit on the minimum nozzle radius. Although radii on the order of 1-5 cm are typical of current designs, source flow laser nozzles with r_i on the order of 0.6 cm have been built and tested.[17]

A number of approximations were used in developing the model, particularly in our treatment of the mixing layer between the fuel and oxidizer streams. These approximations represent an attempt to retain a simple yet physically realistic model for the mixing layer. In this regard, it should be mentioned that our knowledge of the mixing process occurring between the two streams, which enter the laser cavity with pressures that are different by several orders of magnitude, is still quite limited. Careful experimental measurements of mixed zone properties, even for the mixing of inert streams, in typical laser configurations would be extremely valuable.

In this analysis, we have also neglected the effects of the base region between the nozzles on both the lasing kinetics and on the gasdynamics of the laser cavity. Unless purged, the base region can adversely affect lasing performance because of a preponderance of ground state molecules in the slowly recirculating flow of the base. In addition, the pressure mismatch between the base region and the flow exiting the nozzle will, in general, cause the flow to deviate from pure source flow. This latter effect is discussed in some detail in Ref. 6.

Acknowledgments

This work was supported in part by DARPA under Contract DAAK40-78-C-0256, and in part by the Department of the Army under Contract DAAK40-79-C-0136.

References

[1] Cohen, N. and Bott, J. F., "Kinetics of Hydrogen-Halide Chemical Lasers," *Handbook of Chemical Lasers*, edited by R.W.F. Gross and J. F. Bott, John Wiley & Sons, New York, 1976, pp. 33-94.

[2] Thoenes, J., Hendricks, W. L., Kurzius, S. C., and Wang, F. C., "Advanced Laser Flow Analysis Theory and User's Guide," AFWL-TR-78-19, Feb. 1979.

[3] Ramshaw, J. D. and Dukowicz, J. K., "APACHE: A Generalized-Mesh Eulerian Computer Code for Multicomponent Chemically Reactive Fluid Flow," Los Alamos Scientific Lab., Rept. LA-7427, Jan. 1979.

[4]Mirels, H., "Simplified Model of a Continuous Wave Diffusion-Type Chemical Laser—An Extension," *AIAA Journal*, Vol. 14, July 1976, pp. 930-939.

[5]Grohs, G. and Emanuel, G., "Gas Dynamics of Supersonic Mixing Lasers," *Handbook of Chemical Lasers*, edited by R.W.F. Gross and J. F. Bott, John Wiley & Sons, New York, 1976, pp. 263-388.

[6]Patterson, K. E., Batteh, J. H., and Howie, S. S., "A Simple Model for Base Pressure Effects in Source Flow Chemical Lasers," AIAA Paper 82-0400, Jan. 1982.

[7]Shapiro, A. H., *Compressible Fluid Flow*, Vol. 1, Ronald Press, New York, 1953, p. 231.

[8]Williams, F. A., *Combustion Theory*, Addison-Wesley, Reading, Mass., 1965, pp. 37-44.

[9]Polanyi, J. C. and Woodall, K. B., "Energy Distribution Among Reaction Products, VI: $F+H_2$, D_2," *Journal of Chemical Physics*, Vol. 57, Aug. 1972, pp. 1574-1586.

[10]Hall, R. J., "Rotational Nonequilibrium and Line-Selected Operation in CW DF Chemical Lasers," *IEEE Journal of Quantum Electronics*, Vol. QE-12, Aug. 1976, pp. 453-462.

[11]Sentman, L. H., "Rotational Nonequilibrium in CW Chemical Lasers," *Journal of Chemical Physics*, Vol. 62, May 1975, pp. 3523-3537.

[12]Broadwell, J. E., "Effect of Mixing Rate on HF Chemical Laser Performance," *Applied Optics*, Vol. 13, April 1974, pp. 962-967.

[13]Emanuel, G. and Whittier, J. S., "Closed-Form Solution to Rate Equations for an $F+H_2$ Laser Oscillator," *Applied Optics*, Vol. 11, Sept. 1972, pp. 2047-2056.

[14]Mirels, H., "Source Flow Effect on Lineshape," *Applied Optics*, Vol. 20, March 1981, pp. 835-837.

[15]Mirels, H., "Multimode Low-Pressure CW Chemical Laser Performance Including Source Flow Effects," *Applied Optics*, Vol. 20, July 1981, pp. 2379-2388.

[16]Patterson, K. E., Batteh, J. H., and Howie, S. S., "Model for Pure Source Flow Chemical Lasers," AIAA Paper 82-0399, Jan. 1982.

[17]Holloman, M., Directed Energy Directorate, U.S. Army Missile Command, private communications, 1981.

From the AIAA Progress in Astronautics and Aeronautics Series . . .

AEROTHERMODYNAMICS AND PLANETARY ENTRY—v. 77

HEAT TRANSFER AND THERMAL CONTROL—v. 78

Edited by A. L. Crosbie, University of Missouri-Rolla

The success of a flight into space rests on the success of the vehicle designer in maintaining a proper degree of thermal balance within the vehicle or thermal protection of the outer structure of the vehicle, as it encounters various remote and hostile environments. This thermal requirement applies to Earth-satellites, planetary spacecraft, entry vehicles, rocket nose cones, and in a very spectacular way, to the U.S. Space Shuttle, with its thermal protection system of tens of thousands of tiles fastened to its vulnerable external surfaces. Although the relevant technology might simply be called heat-transfer engineering, the advanced (and still advancing) character of the problems that have to be solved and the consequent need to resort to basic physics and basic fluid mechanics have prompted the practitioners of the field to call it thermophysics. It is the expectation of the editors and the authors of these volumes that the various sections therefore will be of interest to physicists, materials specialists, fluid dynamicists, and spacecraft engineers, as well as to heat-transfer engineers. Volume 77 is devoted to three main topics, Aerothermodynamics, Thermal Protection, and Planetary Entry. Volume 78 is devoted to Radiation Heat Transfer, Conduction Heat Transfer, Heat Pipes, and Thermal Control. In a broad sense, the former volume deals with the external situation between the spacecraft and its environment, whereas the latter volume deals mainly with the thermal processes occurring within the spacecraft that affect its temperature distribution. Both volumes bring forth new information and new theoretical treatments not previously published in book or journal literature.

Volume 77—444 pp., 6×9, illus., $30.00 Mem., $45.00 List
Volume 78—538 pp., 6×9, illus., $30.00 Mem., $45.00 List

TO ORDER WRITE: Publications Dept., AIAA, 1290 Avenue of the Americas, New York, N.Y. 10104